Biophysical Chemistry 245 (2019) 6–16

Contents lists available at ScienceDirect

Biophysical Chemistry

journal homepage: www.elsevier.com/locate/biophyschem

DNA recognition by linear indole-biphenyl DNA minor groove ligands

Noa Erlitzki[a], Abdelbasset A. Farahat[a,b], Arvind Kumar[a], David W. Boykin[a], Gregory M.K. Poon[a,c,*]

[a] Department of Chemistry, Georgia State University, Atlanta, GA 30303, USA
[b] Department of Pharmaceutical Organic Chemistry, Faculty of Pharmacy, Mansoura University, Mansoura, Egypt
[c] Center for Diagnostics and Therapeutics, Georgia State University, Atlanta, GA 30303, USA

HIGHLIGHTS

- Non-isohelical heterocyclic cations target DNA with heterogeneous binding modes.
- Dications with a linear indole-biphenyl core bind DNA preferentially as dimers.
- Their mono-cationic analogues bind as monomers to the same DNA.
- Binding modes are strongly sensitive to preferential interactions with co-solutes.
- Charge number and cation substituents determine preference in binding modes.

GRAPHICAL ABSTRACT

ARTICLE INFO

Keywords:
Drug-DNA interactions
DNA minor groove
Heterocyclic dications
Fluorescence
Dimerization
Binding modes

ABSTRACT

Linear heterocyclic cations are interesting DNA minor groove ligands due to their lack of isohelical curvature classically associated with groove-binding compounds. We determined the DNA binding properties of four related dications harboring a linear indole-biphenyl core: the diamidine DB1883, a ditetrahydropyrimidine derivative (DB1804), and their monocationic counterparts (DB1944 and DB2627). These compounds exhibit heterogeneity in binding in accordance with their structures. Whereas the monocations exhibit salt-sensitive 1:1 binding to the duplex 5'-CGCGAATTCGCG-3′ (A_2T_2), the dications show a marked preference for a salt-insensitive 2:1 complex. The two binding modes are differentially modulated by salt and specific non-ionic co-solutes. For both dications, 2-methyl-2,4-pentanediol enforces 1:1 binding as observed crystallographically. Fluorescence quenching studies show self-association without DNA in a relative order that is correlated with preference for the 2:1 complex. The data support a structure-binding relationship in which favorable cation-π interactions drive dimer formation *via* antiparallel stacking of the linear indole-biphenyl cation motif.

1. Introduction

Studies into the properties of DNA-binding ligands inform the design of DNA-targeting drugs and extend our understanding of DNA recognition more broadly. Linear compounds that target the DNA minor groove are of particular interest, as they deviate from the conventional notion of curvature matching that of the groove (isohelicity) as a requirement for high-affinity DNA binding [1,2]. A classic example is the anti-trypanosomal agent CGP 40215A, a linear symmetric diamidine that binds as well as its curved analog Berenil to AT-rich DNA [3,4].

* Corresponding author at: P.O. Box 3965, Atlanta, GA 30303, USA.
E-mail address: gpoon@gsu.edu (G.M.K. Poon).

https://doi.org/10.1016/j.bpc.2018.11.004
Received 26 September 2018; Received in revised form 15 November 2018; Accepted 22 November 2018
Available online 26 November 2018

The diamidine DB921, which harbors a linear benzimidazole-biphenyl core, binds the AT-rich minor groove with ~10-fold higher affinity than its isohelical analog DB911 [5]. Co-crystal structures of these and other compounds with DNA [6,7] all reveal water molecules bridging the gaps between ligand and minor groove. These examples establish the ability of non-isohelical compounds of diverse structures to bind to DNA and a role for hydration in facilitating complementarity with the DNA minor groove.

More recently, the co-crystal structures of the asymmetric linear dications DB1804 and DB1883 with DNA were reported [8]. DB1883 is the indole-biphenyl analog of DB921, while DB1804 is a carbocyclic derivative of DB1883. Both DB1883 and DB1804 bind AT-rich DNA with similar affinities as DB921. With the report of a mono-amidine derivative of DB1883 exhibiting weak binding to the same DNA target, we became interested in the structure-affinity relationships between charge density and substitution at the termini of these linear minor groove binders. In our investigations, we found that these compounds were heterogeneous in their DNA binding properties. Both DB1804 and DB1883, but not their monocationic counterparts, form 2:1 complexes in preference over the 1:1 complexes observed in co-crystal structures with the same AATT-bearing DNA target. The discrepant binding properties exhibited by the same compounds and DNA between solution and crystal suggest that preferential interactions with other solutes play an important role in directing the binding modes of these minor groove ligands. While “non-standard” binding modes of minor groove-binding compounds and their DNA sequence requirements have been extensively described [9], the physical chemistry of this behavior, which requires experimental characterization of the properties of the unbound compounds, is less well understood. We therefore interrogated a set of four related indole-biphenyl compounds consisting of DB1804, DB1883, DB2627, and DB1944 (Fig. 1) in both their DNA-bound and free states. DB2627 and DB1944 are the monocationic derivatives of DB1804 and DB1883, wherein the amidine and tetrahydropyrimidine (THP) at the phenyl ends are uninstalled. The data show a structure-binding relationship for an indole-biphenyl cation core that is sensitive to the DNA minor groove as well as the physicochemical environment in the absence and presence of DNA.

2. Materials and methods

2.1. Compounds and DNA

The syntheses of DB1883, DB1804, and DB1994 have been previously described [8]. The synthesis of DB2627 is detailed in *Supplemental Methods*. DNA oligonucleotides encoding A_2T_2 and A_2CGT_2 (Fig. 1) were synthesized by Integrated DNA Technologies (Coralville, IA). Lyophilized DNA was dissolved at 1 mM in 10 mM TrisHCl (pH 7.5) containing 1.0 M NaCl and then dialyzed (MWCO 3.5 kDa) extensively against 10 mM TrisHCl (pH 7.5). Duplex DNA concentration was measured by UV absorption at 260 nm using the nearest-neighbor extinction coefficients 191,511 $M^{-1}\,cm^{-1}$ for A_2T_2 and 190,127 $M^{-1}\,cm^{-1}$ for A_2CGT_2. All other reagents were obtained at ACS grade or higher purity and used without further purification.

2.2. Binding experiments

DNA binding at equilibrium was monitored by steady-state polarization of the intrinsic blue fluorescence of the compounds as previously described [10,11]. In brief, each compound was titrated with DNA in 10 mM TrisHCl (pH 7.5) with or without other co-solutes as stated in the text and measured using a Perkin-Elmer LS 55 instrument. The excitation and emission maxima were established at 328/456 (DB1883), 338/454 (DB1944), 337/438 (DB2627), or 320/438 nm (DB1804). Steady-state anisotropy was computed using a grating factor as determined under the conditions of each measurement. With excitation and emission slit widths of 15 and 20 nm centered at these wavelengths, each compound was sampled at the lowest concentration sufficient to acquire signal for anisotropy measurements after blank subtraction: 50 nM for DB1883, 20 nM for DB1944, 10 nM for DB2627, 20 nM for DB1804, unless otherwise indicated in the text.

2.3. Steady-state fluorescence quenching

Each compound was titrated at a constant concentration of 200 nM in water with NaI, acrylamide, and nicotinamide. Total intensity and steady-state anisotropy at λ_{max} were adjusted for volume changes, blank-subtracted, and analyzed by linear regression.

2.4. Data analysis

The signal from DNA titration experiments represented the fractional bound compound (F_b), scaled by the limiting anisotropies of the ensemble of n (typically 1 or 2) bound states $\langle r_i \rangle$ and unbound state $\langle r_0 \rangle$ as follows:

$$\langle r \rangle = F_b \left(\sum_{i=1}^{n} \langle r_i \rangle - \langle r_0 \rangle \right) + \langle r_0 \rangle = F_b \sum_{i=1}^{n} \Delta r_i + \langle r_0 \rangle \quad (1)$$

F_b is described empirically by the Hill equation or a mechanistic binding model as described in the text with total DNA concentration

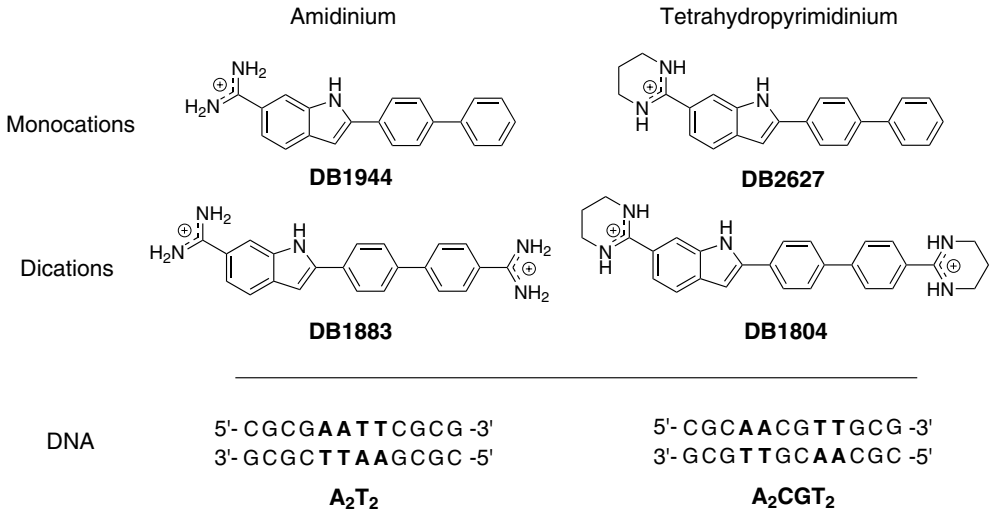

Fig. 1. Minor-groove binding ligands and target DNA used in this study. The minor-groove binders consist of the linear indole-biphenyl amidine DB1944 and three interrelated compounds, shown in the ionization state expected at pH 7.5. DB2627 is the tetrahydropyrimidine (THP) analogue. DB1883 and DB1804 are dicationic variants of DB1944 and DB2627, respectively. The two DNA targets are the standard AATT dodecamer (A_2T_2) and an isomeric sequence in which the AT-tract is interrupted (A_2CGT_2).

taken as independent variable. For salt-dependent analysis, mean ionic activity was calculated from molal concentration and literature values of the mean ionic activity coefficient $a_{\pm}$ in water [12]. The dependence of DNA-binding affinities on $a_{\pm}$ is analyzed in terms of polyelectrolyte theory to estimate the number of neutralized DNA backbone phosphates Z from the net number of displaced ions $n_{\pm}$:

$$-\frac{\log K_D}{\log a_{\pm}} = n_{\pm} = \psi Z = \left(\psi_{\infty} - \frac{2.53}{N}\right)Z \quad (2)$$

where ψ reflects screening and condensation interactions between backbone phosphates in B-DNA and their ion atmosphere [13]. The assigned value of $\psi = 0.67$ includes an end-effect correction for our $N = 12$ bp oligonucleotide duplexes relative to polymeric DNA ($\psi_{\infty} = 0.88$) [14].

3. Results

Binding to the target duplex A_2T_2 in solution was determined at equilibrium by titration with DNA *via* the large change in anisotropy of the intrinsic blue fluorescence of the compounds. This technique, which obviates the need for extrinsic labeling or immobilization of the DNA, reverses the more common approach of titrating the DNA with compound. The titrations were designed such that DNA concentration was varied over five or more decades while keeping the dilution of compound to less than ~5%, which was sufficiently fixed for one-dimensional analysis [11]. At pH 7.5, as a function of increasing NaCl concentration from 0.010 to 0.750 M, the titration profiles for DB1804 exhibited an increasingly biphasic appearance (Fig. 2A), while those for the other compounds remained monophasic (Fig. 2B to D). As a first step to parameterize the two binding modes for DB1804, we fitted the data empirically with a sum of two Hill equations:

$$F_b = f\frac{c^{n_{H,1}}}{K_{D,1}^{n_{H,1}} + c^{n_{H,1}}} + (1-f)\frac{c^{n_{H,2}}}{K_{D,2}^{n_{H,2}} + c^{n_{H,2}}} \quad (3)$$

where $n_{H,i}$ is the Hill coefficient and $K_{D,i}$ is the DNA concentration at half maximal occupancy for binding mode $i = 1$ or 2. The scaling factor f represents the fractional contribution to the total anisotropy change from each binding mode. To statistically infer the extent to which the salt-dependent binding profiles exhibited biphasic character, we compared the fits of each dataset by Eq. (3) (with f floating) relative to a single term (f fixed at 1) using the Fisher F-test on the residual sums of squares. Across the full range of NaCl concentrations tested, the two-term Hill model afforded significantly better fits to the DB1804 data than a single term ($p < 0.05$; Table S1, Supplemental Data). Thus, the binding properties of DB1804 (the THP dication) exhibited two spectroscopically distinguishable binding modes at equilibrium. In contrast, titration profiles for its mono-THP counterpart (DB2627) as well as the di- (DB1883) and mono-amidine (DB1944) were monophasic across the entire salt range as confirmed by F-testing (Table S1).

3.1. Linear dications exhibit salt-sensitive and salt-insensitive binding modes

Examination of the empirical affinities ($K_{D,i}$) revealed distinct trends in salt dependence for the four related compounds (Fig. 3). For DB1804, the high-affinity binding mode ($K_{D,2}$) exhibited no salt dependence, while the low-affinity binding mode ($K_{D,1}$) varied linearly with mean ionic activity with a log-log slope of -0.63 ± 0.10. For the diamidine DB1883, the titration curves were insensitive to salt, similar to the high-affinity mode of DB1804. We considered the possibility that the high-affinity modes might appear to be insensitive to salt due to titrant depletion, *i.e.,* binding was tight such that $K_{D,1}$ reflected the (fixed) compound concentrations in the titrations rather than binding affinities. However, the apparent dissociation constants corresponding to the high-affinity mode ($K_{D,2}$) were ~10-fold lower than the concentrations of the dications used (20 nM for DB1804, 50 nM for DB1883). Moreover, the dissociation constants for both dications agree closely with values measured by surface plasmon resonance, an altogether different experimental configuration [8]. Therefore, the apparent salt insensitivity could not be significantly attributed to depletion. We concluded that the salt insensitivity of the single binding mode of DB1883 and the high-affinity mode of DB1804 was intrinsic to their binding properties.

For the monocations, the THP (DB2627) bound A_2T_2 with ~3-fold higher affinity than the amidine DB1944, and both compounds gave identical salt dependence at -0.60 ± 0.10 (DB1944) and -0.64 ± 0.03 (DB2627) in log-log slope. Interpreting this slope by polyelectrolyte theory [13], given by Eq. (2) for oligonucleotides [14], binding of A_2T_2 by DB2627 and DB1944 corresponded to the neutralization of one DNA phosphate.

The salt dependence data suggested that the salt-insensitive high-affinity binding mode for DB1804 to A_2T_2 was similar to DB1883. Likewise, the salt-sensitive low-affinity mode for DB1804 was similar to the two monocations. Since the titrations used DNA as titrant, increasing DNA concentration was expected to drive the equilibria in the direction of *decreasing* stoichiometric order with respect to compound. Combining these clues, we hypothesized that the biphasic binding by DB1804 reflected a distribution between two distinct stoichiometric complexes with DNA. To test this hypothesis, we determined the stoichiometry of the apparent complexes for all four compounds under depleting conditions at the low NaCl concentration of 5 mM [Fig. 4]. The binding curves revealed that the high-affinity binding mode for DB1804 and the single binding mode for DB1883 represented the dications in 2:1 excess to DNA, while their monocationic counterparts exhibited equimolar binding. To rule out the formal possibility that these complexes might consist of DNA at multiple equivalents, we probed DB1804-bound A_2T_2 by size-exclusion chromatography (Fig. S1, Supplemental Data). At DNA concentrations sufficient for UV detection (5 μM), we detected no species consisting of two or more A_2T_2 duplexes. The evidence therefore showed that the spectroscopically distinct modes of DB1804 binding to A_2T_2 both involved a single duplex.

To mechanistically analyze the binding properties of DB1804, we modeled its titration profiles according to Scheme I, where the equilibria are written (from left to right) in the opposite direction as our titrations. K_1 and K_2 are the intrinsic stepwise dissociation constants for the 1:1 (low-affinity) complex and 2:1 (high-affinity) complex, respectively. The functional form of Scheme I is given in *Supplemental Methods*. As shown in Fig. 5A, Scheme I described DB1804 binding to A_2T_2 across the full range of NaCl concentrations tested and captured the distinct salt dependence of the 1:1 and 2:1 complexes. To generalize the salt-dependence data, we tested the effect of Na_2SO_4 in place of NaCl on DB1804 binding. The titration profiles for Na_2SO_4 showed similarly biphasic properties that were also described by Scheme I, although the two binding modes were not as well-resolved as with NaCl at matching Na^+ concentrations. However, when cast as a function of mean ionic activity [12], perturbation of binding by Na_2SO_4 fell in line with the data for NaCl (Fig. 5B). Thus, the salt-induced divergence of the two binding modes of DB1804 was consistent with an equilibrium distribution of a 2:1 and a lower-affinity 1:1 complex, only the latter of which was sensitive to the ionic environment (-0.75 ± 0.18 in log-log slope). Moreover, the independence of this perturbation from anion identity confirmed that release of condensed DNA counter-ions, as described by polyelectrolyte theory, accounted for the disposition of ions in salt-sensitive binding.

Two features of Scheme I are of note. First, since the final state in the titration was the 1:1 complex, the model assigned a higher steady-state fluorescence anisotropy to the 1:1 complex than the 2:1 complex in the titrations (on the order of 10%). Second, the equilibrium constants are formulated with unbound compound as monomers. While it is possible to incorporate additional equilibria for the self-association of

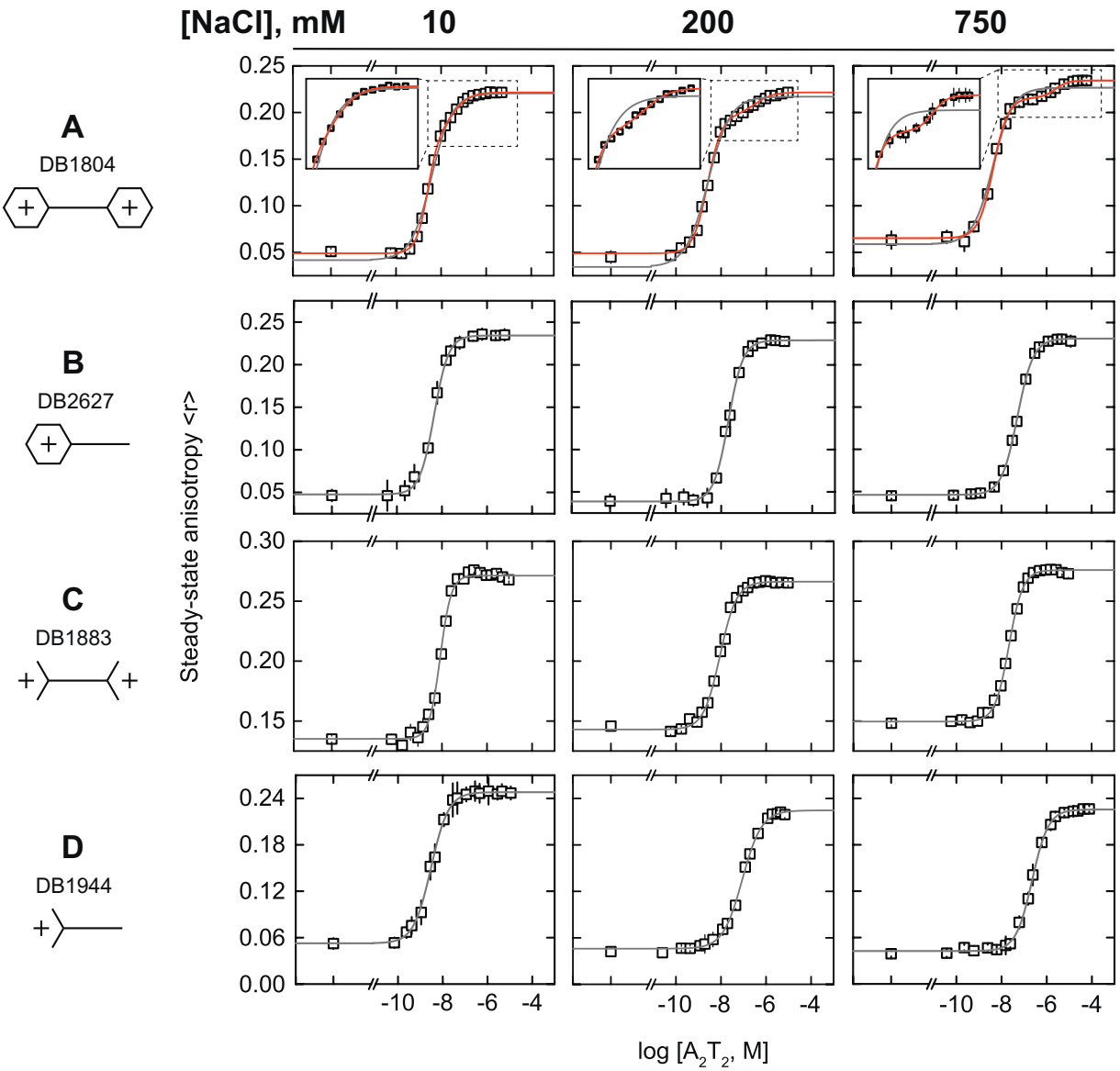

Fig. 2. NaCl unmasks two distinct binding modes for the ditetrahydropyrimidine DB1804. Rows A to D show representative A_2T_2-into-compound titrations for each species in the presence of 10 to 750 mM NaCl. *Curves* represent fits by either a one- (gray) or two-term Hill equation (red) as given in Eq. (3). Compounds were present at 10^{-9}–10^{-8} M as described in *Materials and Methods*. (For interpretation of the references to colour in this figure legend, the reader is referred to the web version of this article.)

the unbound compound, the parameters for these interactions, such as the anisotropies of the DNA-free species, are not well defined by the titration data. Although these details were not included in Scheme I, the scheme afforded a satisfactory fit to the experimental data and captured the salient details of the system, namely the salt-sensitive low-affinity binding mode and the salt-insensitive high-affinity binding mode.

3.2. The binding modes of DB1804 are DNA sequence-specific

Having established a 2:1 complex as the high-affinity binding mode for DB1804 to A_2T_2, we asked whether this behavior was specific to the DNA sequence (Fig. 6). To address this question, we permuted the dodecameric A_2T_2 to generate an isomeric sequence harboring 5′-AACGTT-3′ (A_2CGT_2; Fig. 1). DB1804 bound A_2CGT_2 more weakly than A_2T_2 and exhibited more than one binding mode, although the corresponding anisotropies did not coincide. At 10 mM Na^+, the high-affinity mode for A_2CGT_2 was comparable to that for A_2T_2, but the low-affinity mode was ~100-fold weaker. In contrast with A_2T_2, the high-affinity mode for A_2CGT_2 was salt-sensitive, becoming ~100-fold weaker in 200 mM Na^+. In addition to the apparent affinities, the anisotropies associated with the binding modes for A_2CGT_2 progressively diverged from those associated with A_2T_2 with increasing Na^+ concentration. These changes suggested DNA-dependent dynamics, photophysical properties of different binding modes or, more likely, the development of additional nonspecific modes with A_2CGT_2. Moreover, as the salt dependence of binding was described by DNA counter-ion condensation over the experimental salt concentrations (*vide supra*), the observed sequence specificity was expected to be general with respect to cation identity [15]. In summary, the two binding modes observed with the A_2T_2 site were sequence-specific and therefore relevant to this high-affinity DNA that dications are generally known to target.

3.3. The binding modes of DB1804 are sensitive to inhibition by netropsin

To further define the high- and low-affinity DNA-bound states of DB1804, we challenged the DB1804:A_2T_2 complexes with netropsin, a

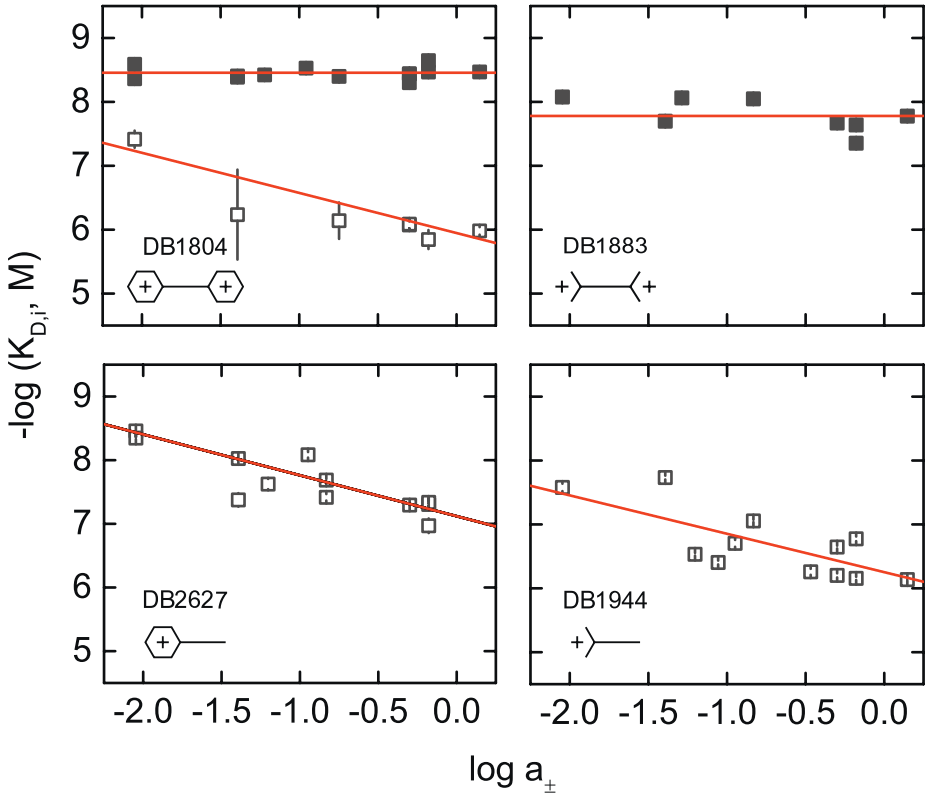

Fig. 3. Salt dependence of DNA binding by indole-biphenyl mono- and dications. Empirical dissociation constants of titration curves obtained at 10 to 750 mM NaCl were estimated by a Hill analysis according to Eq. (3). DB1804, DB1883, DB2627, DB1904. Closed and open *symbols* refer respectively to the apparent high- and low-affinity modes, *i.e.*, $K_{D,1}$ and $K_{D,2}$ in Eq. (3), observed with DB1804 that were absent with the other compounds.

well-established minor groove ligand for A_2T_2. Competition titrations with (non-fluorescent) netropsin were performed at DNA concentrations corresponding to saturated and various levels of sub-saturated binding by DB1804 in 10 or 750 mM NaCl (Fig. 7). Displacement of DB1804 from A_2T_2 by netropsin was indicated by a decrease in the

$$\text{DNA} \overset{K_1}{\rightleftharpoons} \text{DB} : \text{DNA} \overset{K_2}{\rightleftharpoons} \text{DB}_2 : \text{DNA}$$

Scheme I. Mechanistic model for DB1804 binding to A_2T_2.

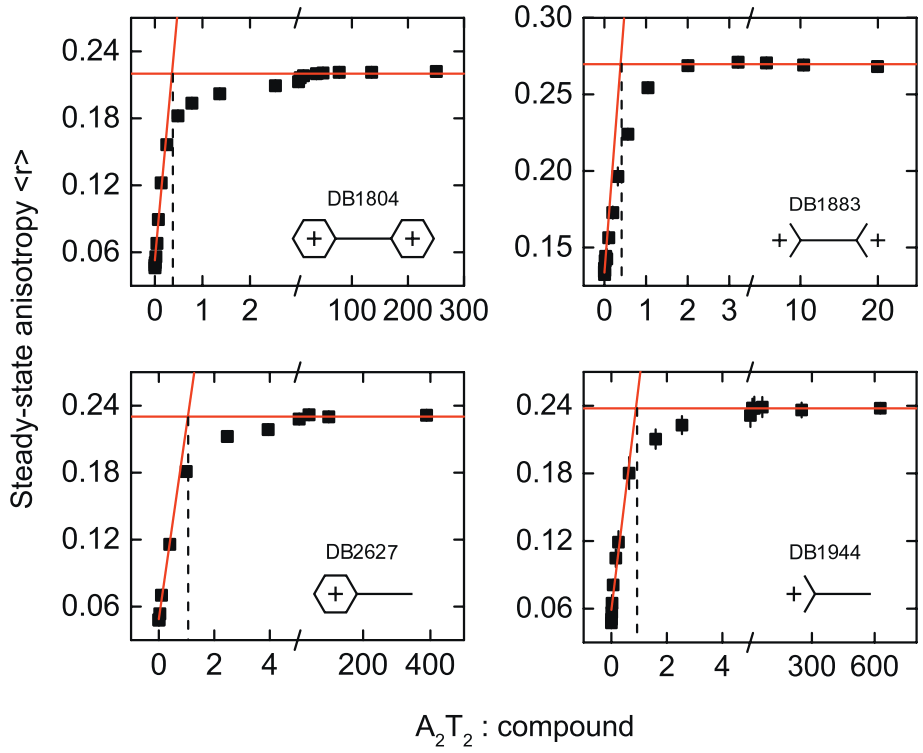

Fig. 4. Stoichiometry of A_2T_2-bound complexes of linear cations. Binding was measured at 5 mM NaCl. Compound concentrations ranged from 10 to 140 nM.

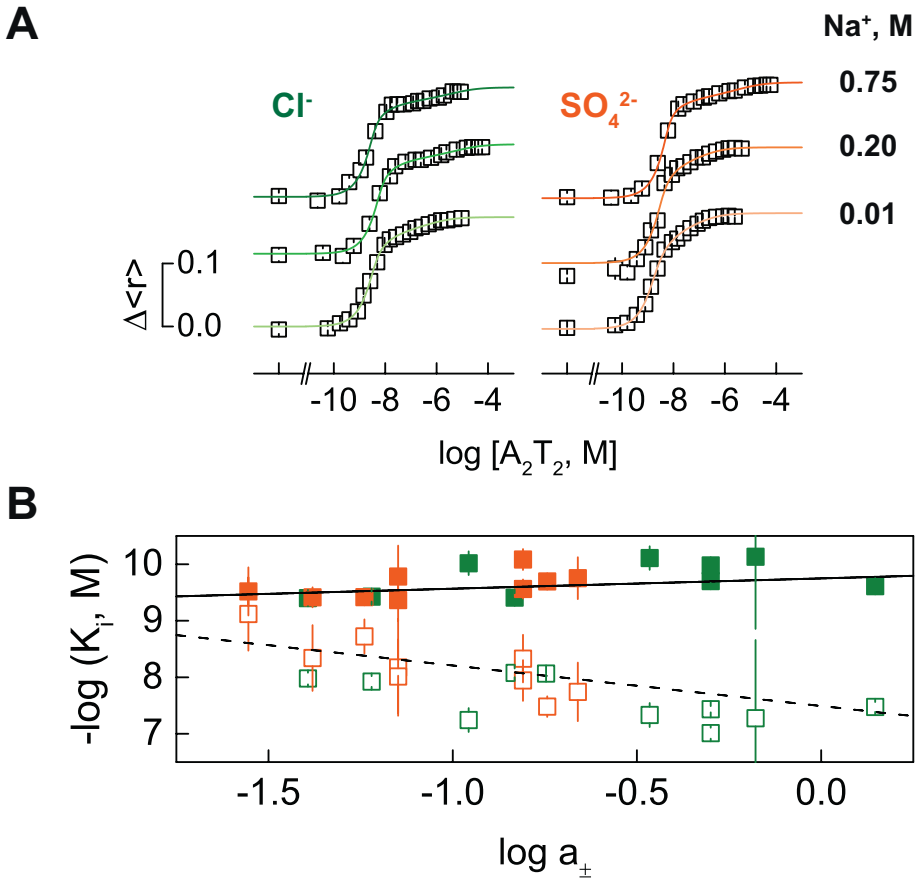

Fig. 5. DNA recognition by DB1804 is mechanistically described by an equilibrium distribution of 2:1 and 1:1 complexes. A, Titration data for DB1804 for the three NaCl concentrations (green) shown in Fig. 2A was globally fitted with Scheme I with $\Delta < r >$ for the two complexes shared, *c.f.* Eq. (1). DNA titrations in the presence of Na_2SO_4 instead of NaCl, shown here in orange at matching Na^+ concentrations, were also fitted with this model. *Curves* are offset vertically for presentation. B, Salt-dependence of the dissociation constants for the low- (open symbols) and high-affinity (closed symbols) transitions obtained by fitting the binding data to Scheme I. Lines of best fit for K_1 (dashed) and K_2 (solid) were obtained by globally fitting the data for NaCl (green) and Na_2SO_4 (orange). (For interpretation of the references to colour in this figure legend, the reader is referred to the web version of this article.)

apparent anisotropy of DB1804. As expected for the salt-sensitive binding of netropsin to A_2T_2 [16], it competed for the DNA more strongly at the low salt condition. At all DB1804 concentrations, netropsin was initially observed to displace the bound DB1804 from the DNA. Interestingly, control experiments showed an interaction between DB1804 and netropsin above 10^{-6} M concentration of the latter *in the absence of DNA*. Though this unexpected behavior obscured a full competition profile, it remained apparent that both binding modes could be inhibited by netropsin and supported the minor groove as the binding site of DB1804 in both modes.

3.4. Preferential interactions with co-solutes modify the binding modes of DB1804

To better understand the physicochemical basis of the different binding modes exhibited by DB1804, we examined the effects of non-ionic co-solutes on its DNA binding equilibria. We initially focused on dimethyl sulfoxide (DMSO) and nicotinamide, two common solubilizing agents for low-molecular weight compounds. At up to 20% *v*/v DMSO (2.8 m), the biphasic transition persisted, but the apparent affinities for both binding modes were attenuated (Fig. S2A, Supplemental Data). In

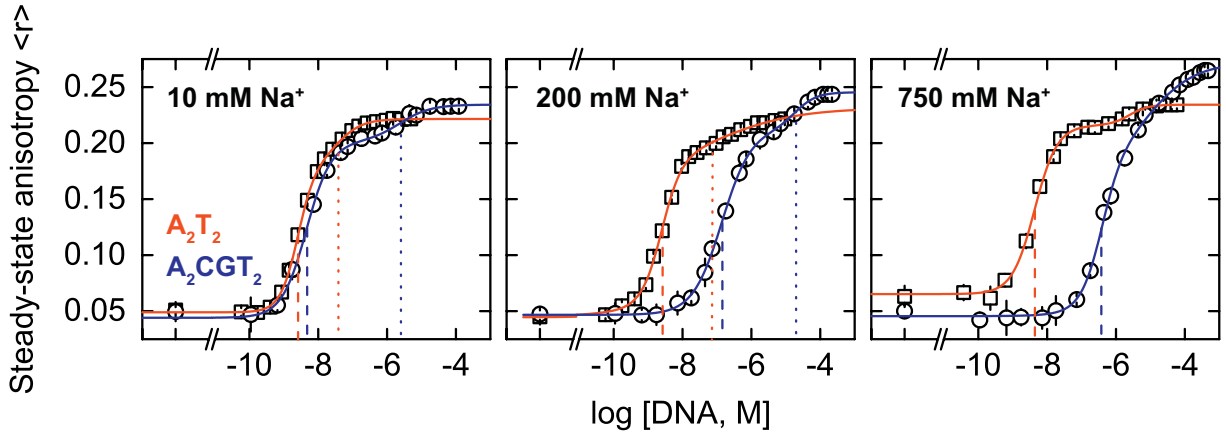

Fig. 6. The 2:1 and 1:1 binding modes exhibited by DB1804 are sequence-specific. DB1804 was titrated with the interrupted AT-tract (A_2CGT_2; circles, blue) in 10, 200, and 750 mM NaCl. The data is plotted alongside corresponding data for the specific site A_2T_2 from Fig. 2A (squares, red) to facilitate comparison. *Curves* represent empirical fits by the two-term Hill equation, Eq. (2). $K_{D,1}$ and $K_{D,2}$ are indicated by dashed and dotted drop lines, respectively. At 750 mM NaCl, additional binding modes appeared likely for A_2CGT_2. (For interpretation of the references to colour in this figure legend, the reader is referred to the web version of this article.)

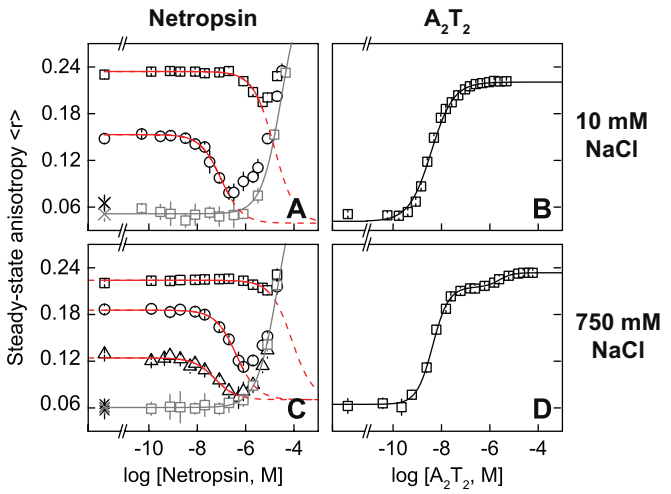

Fig. 7. Inhibition of A_2T_2-bound DB1804 by netropsin. Netropsin was titrated into A_2T_2-bound DB1804 at 10 mM (top) and 750 mM NaCl (bottom). DB1804 was present at 20 nM in all cases. At both Na^+ concentrations, DB1804 was complexed with 2 nM (triangles), 8 nM (circles), and 700 nM DNA (squares). Binding between DB1804 and netropsin was detected above $\sim 10^{-6}$ M netropsin in the *absence* of DNA (gray). Unbound DB1804 is marked by ×. Data from Fig. 2A showing A_2T_2 titrations at the corresponding salt concentrations is shown in the panels at right for comparison.

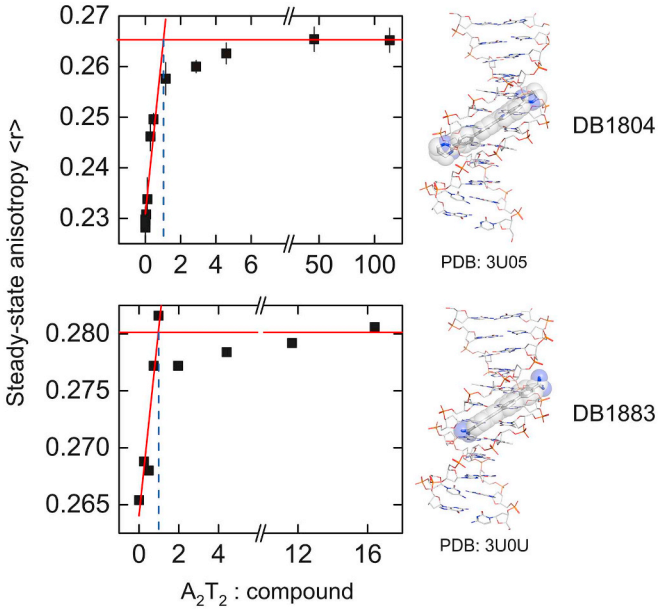

Fig. 8. The cryo-protectant 2-methyl-2,4-pentainediol enforces 1:1 binding by linear dications. Binding of A_2T_2 to 100 nM DB1804 or 740 nM DB1883 at 750 mM NaCl was measured in the presence of 50% MPD as used in the crystal structures. The error bars used during fitting, which average ± 0.05, have been omitted in Panel B for clarity. The small change in anisotropy for DB1883 compared to DB1804 reflects the higher unbound anisotropy associated with this compound (*c.f.*, Fig. 2). Stoichiometric analyses indicate equimolar complexation of each compound with A_2T_2 under these conditions. At right, the crystal structures for A_2T_2-bound DB1804 (PDB ID: 3U05) and DB1883 (PDB ID: 3U0U) show the two bound species forming 1:1 complexes.

contrast, nicotinamide at up to 0.10 M (0.09 m) exerted opposing effects on the two binding modes, slightly favoring the high-affinity mode while significantly destabilizing the low-affinity mode (Fig. S2B, Supplemental Data). The qualitatively different effects of DMSO and nicotinamide on the two binding modes indicated that they arose from specific preferential interactions with the co-solutes and were not due to viscosity or colligative effects such as hydration alone.

In light of the 1:1 complexes observed in co-crystal structures of DB1804 and DB1883 with A_2T_2, and the sensitivity of the binding modes to co-solutes, we considered whether crystallization conditions might contribute to the different binding behaviors observed for these dications in solution. As the reported crystallization conditions [8] employed 2-methyl-2,4-pentanediol (MPD) as a cryo-protectant and precipitant at up to 50% v/v during equilibration, we performed titrations of DB1804 and DB1883 with A_2T_2 in the presence of 50% v/v MPD. Although the high viscosity of MPD strongly perturbed the observed anisotropy of both compounds, it gave equimolar binding by both DB1804 and DB1883 at 750 mM Na^+ (Fig. 8). MPD therefore suppressed the 2:1 complex and enforced the alternative 1:1 complex, even under high-salt conditions in which it would be otherwise disfavored, to yield the stoichiometry seen in the co-crystal structures with A_2T_2.

3.5. Linear dications self-associate in the absence of DNA

An important feature of the dications not directly addressed by the binding experiments was whether the dications dimerize in the absence of DNA. In one possibility, dication monomers are induced to dimerize onto DNA. Alternatively, unbound dications assemble into pre-formed dimers (or other oligomers) that persist upon binding to DNA. A pre-organized dimer would decrease the entropic barrier for forming the 2:1 complex, offering a possible explanation for the higher affinity of this binding mode relative to the 1:1 complex. To probe whether the compounds self-associate in the unbound state, we determined the effect of quenching agents on the intrinsic fluorescence of each compound. We tested three chemically distinct quenchers (NaI, acrylamide, and nicotinamide) at a common compound concentration of 200 nM to allow for sufficient fluorescence detection upon quenching. We analyzed the decay in total fluorescence intensity upon incremental additions of quencher according to the Stern-Volmer relationship (Fig. 9A to C):

$$\frac{F_0}{F} = \frac{\tau_0}{\tau} = 1 + K[\mathrm{Q}] \tag{4}$$

where F_0 and F represent fluorescence in the absence and presence of quencher Q, and the (positive) slope K is the Stern-Volmer constant K_{SV} in the case of dynamic quenching or the association constant K_a in the case of static quenching. To differentiate between dynamic and static contributions to the observed intensity quench, we simultaneously determined the steady-state anisotropy at each concentration step as a proxy for fluorescence lifetime, τ. The two quantities are related by the Perrin equation:

$$\frac{1}{r} = \frac{1}{r_0} + \frac{RT}{r_0 \eta V}\tau \tag{5}$$

where r_0 is the limiting anisotropy, R is the gas constant, T is the absolute temperature, η is viscosity, and V is the molar hydrated volume. Dynamic quench is modeled by substitution of the Stern-Volmer relationship into τ [17]:

$$\frac{1}{r} = \frac{1}{r_0} + \frac{RT}{r_0 \eta V}\frac{1}{1 + K_{SV}[\mathrm{Q}]} \tag{6}$$

As Fig. 9D to F show, the anisotropies exhibited small changes with no systematic trends, even in cases where fluorescence intensity changed significantly. To constrain the analysis, we used a relatively low and narrow range of quencher concentrations (up to 6 mM) to minimize viscosity and preferential hydration effects on the observed anisotropies. As it was then improbable that any change in viscosity and hydration would compensate so similarly for the three chemically disparate quenchers if K_{SV} were substantial, we concluded that the weak dependence of the observed anisotropy on quencher concentration reflected a small K_{SV}. We therefore reject collisional relaxation of the

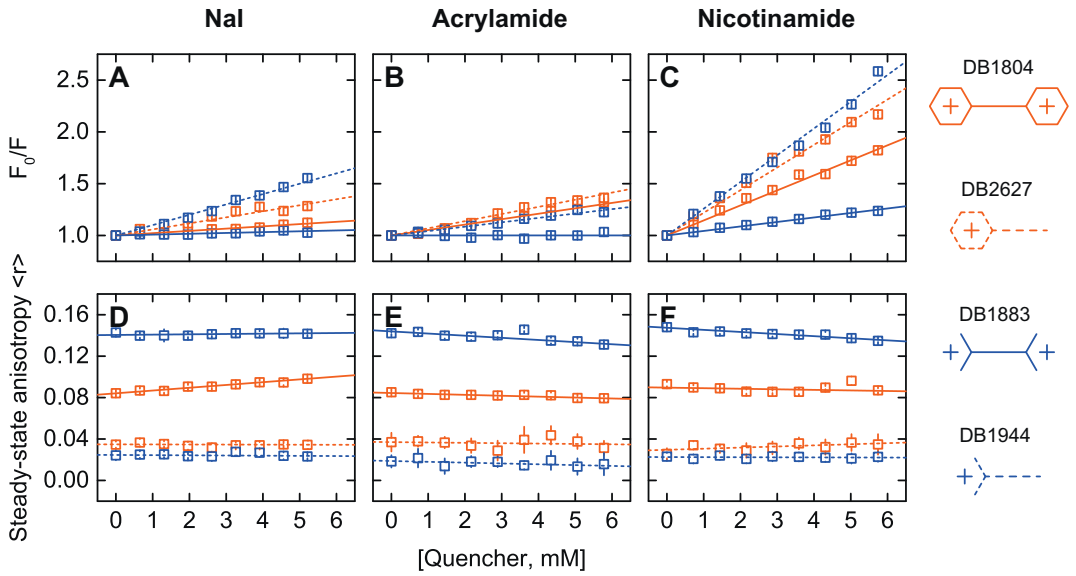

Fig. 9. Steady-state fluorescence quenching of linear indole-biphenyl cations in the absence of DNA. Total fluorescence intensity (A to C) and steady-state anisotropy (D to F) were measured for each compound at 200 nM in the presence of NaI, acrylamide, and nicotinamide.

excited state as a significant contributor to the intensity quench, which must therefore represent quencher-specific interactions of ground state species at equilibrium (static quench).

Having established preferential interactions of the ground-state compounds with the quenchers as the basis of the intensity quench, several overarching observations presented themselves. First, nicotinamide was the most efficient quencher for each compound, consistent with its reputation as a hydrotrope with strong preferential interaction properties. Second, regardless of quencher identity, each monocation exhibited a higher K_a (*i.e.*, was more sensitively quenched) than its dicationic analogue. Since it was improbable that the additional charge in the dications would result in less favorable interactions with all three chemically distinct quenchers, we interpreted this behavior as self-association of the dications. Thus, dimeric DB1804 and DB1883 presented significantly less accessible surface areas (or lower effective concentrations) to the quenchers. Third, the diamidine showed a significantly larger difference in intensity quench relative to the monoamidine than the corresponding THPs. Along the same line of reasoning, we interpreted this difference in terms of a stronger preference by the unsubstituted dications for self-association (*i.e.,* DB1883 > DB1804). As A_2T_2 induced 1:1 binding by DB1804, but not DB1883 (Fig. 3), the relative tendency of the linear dications to self-associate appeared to correlate with their preference for 2:1 binding over the 1:1 complex.

4. Discussion

The iconic binding mode of minor groove ligands, originally observed in the co-crystal structure of netropsin and A_2T_2 [18], is insertion as a monomer deep into the minor groove of duplex B-DNA, usually with a strong preference for AT-rich regions. Depending on the DNA sequence context, other binding modes have also been described. For example, netropsin binds in two molar equivalents to the minor groove of the self-complementary duplex C_5I_5 as an end-to-end dimer [19]. More subtle are thermodynamically or spectroscopically distinguishable netropsin complexes with AT-rich DNA of different configurations, such as sequence variations [20,21] or the presence of a hairpin [22]. Beyond the double helix, netropsin also binds the minor groove of a DNA triplex [23,24]. Reciprocally, specification of binding mode results in conformational selection in the bound DNA, in some cases with dramatic effect [25,26].

Beyond netropsin, DNA-dependent binding modes have also been described among designed minor groove binders. For example, furamidine (DB75, a diphenylfuran diamidine) and related analogs can intercalate or bind to the minor groove of duplex DNA depending on sequence and the relative positions of the substituents in the compounds [27]. DB293 (a phenyl-furan-benzimidazole diamidine) binds to A_2T_2 as a monomer but to mixed (*e.g.*, 5′-ATGA-3′) sequences cooperatively as a stacked antiparallel dimer [28,29]. DB1003, a difuranbenzimidazole derivative of DB293, binds 5′-AATT-3′ as a monomer but 5′-TTAA-3′ as a positively cooperative dimer [30]. The present compounds based on the indole-biphenyl scaffold add to the growing diversity of DNA recognition by low-MW ligands and highlight a role for interactions of the compounds in the unbound state in modulating the selectivity of one binding mode over another.

4.1. Structural determinants of binding mode selection by linear indole-biphenyl cations

The four compounds examined in this study constitute an internally consistent set of analogues from which the structural bases of the multiple binding modes may be inferred. In dilute solution, the dications DB1804 and DB1883 preferentially bind AT-rich DNA as dimers. In the case of DB1804, the dimer succumbs to a 1:1 complex when DNA is in large excess. While the high-affinity 2:1 complex is salt-insensitive, the low-affinity 1:1 complex is destabilized with increasing Na^+ concentration. Thus, for DB1804, the titrations become increasingly biphasic with increasing salt due to the differential sensitivity of the two binding modes to bulk salt concentrations. In the case of DB1883, the corresponding low-affinity mode is presumably too low in affinity to detect at the highest concentration of DNA used (10^{-4} M).

The binding modes exhibited by the dications DB1804 and DB1883 in solution are not reflected in their crystal structures, which consist only of 1:1 complexes. In contrast, DNA binding by their monocationic analogs occurs exclusively as 1:1 complexes. The relationship between the two pairs of amidines (DB1883/DB1944) and THPs (DB1804/DB2627) pose an interesting contrast with an earlier study on DB183 and DB185 [31]. DB185 is a dibenzimidazole-phenyl diamidine that binds 5′-TTAA-3′ as a monomer while DB183, a monocationic derivative in which the phenyl end is replaced by an (uncharged) hydroxyl, targets the same site as a positively cooperative dimer. The *linear* indole-biphenyl compounds in this study also demonstrate a clear

relationship between charge number and dimeric binding but in a manner opposite the *isohelical* pair DB183/DB185. Examples are therefore accumulating that suggest charge number as a parameter for multiple binding modes by heterocyclic cations in the DNA minor groove.

The fluorescence quenching data indicate that both of the dications self-associate at low concentrations in the absence of DNA to a significantly higher extent than the monocations. Structurally, the aromatic indole-biphenyl core suggests a stacking mechanism for dimer formation. The major driving force for stacking, which includes a favorable entropic component due to hydrophobic dehydration of stacked surfaces, should scale with the removal of solvent-accessible surface area. If one side of the indole-biphenyl core becomes inaccessible to solvent in a stacked dimer, stacking would exclude 225 $Å^2$ of surface area per monomer in the dimer. Assuming that the π-stacked termini remain fully solvent-accessible, this reduction represents a lower limit of 26% and 32% of the total solvent-accessible surface area of DB1804 (di-THP) and DB1883 (diamidine), respectively. However, the monocations DB2627 and DB1944 are similar in aromaticity to their dicationic counterparts, differing from DB1804 and DB1883 only in the absence of a cationic terminus. Some charge-based interactions must therefore provide the additional driving force to favor the dicationic dimers over their monocationic counterparts.

Given the propensity of indoles and phenyl rings to engage in cation-π binding, the data suggest a role for cation-π stabilization in the self-association of dicationic compounds. Thus, one might envision an anti-parallel stacked dimer in which the cation at the phenyl end of one dication stabilizes the π interactions near the indole end of another (Fig. 10A). Experimental studies with model low-MW compounds estimate the free energy contribution of single cation-π stack to be on the order of 10 kJ/mol at 25 °C, equivalent to 1 to 2 hydrogen bonds in liquid water [32]. Each dication dimer contains two distinct cation-π stacks. The steric complementarity and symmetry of the linear dications arranged in an antiparallel configuration would further favor association.

Cation-π stacking explains why the cation at the phenyl end is essential for dimer formation: the charge at the indole end is off-axis relative to the linear aromatic core and cannot achieve similar alignment without steric or charge clashes (Fig. 10B). Monocations harboring substituents at the phenyl end are therefore expected to behave similarly to the non-substituted monocations DB2627 and DB1944. The cation-π model also accounts for the stronger dimeric preference of the diamidine (DB1883) over the di-THP (DB1804), as the π-interacting charge density would be attenuated by the carbocyclic ring in DB1804. Finally, cation-π stacking provides a basis for the dimer as a self-limiting unit that does not readily associate into insoluble aggregates, as attested by the solubility of the dications up to 10^{-4} M in aqueous solution. Indeed, the *requirement* for charge in dimerization by these linear dications contrasts with, for example, the heterocyclic polyamides for which aggregation is inhibited by increasing charge density [33].

Given the stacked-dimer model of minor groove occupancy proposed for other heterocyclic dications such as DB293 and DB183 [28–31], a dimeric dication in the unbound state may also be related to its DNA-bound conformation in the 2:1 complex. Structural consistency between the DNA-free and DNA-bound dimers would account for: 1) the absence of a 1:1 complex for DB1883 due to its preference for the dimeric state relative to DB1804, and 2) the absence of 2:1 binding by the monocations. The stacked dimer also presents a plausible symmetry argument for a lower apparent anisotropy (increased dynamics) for the 2:1 complex relative to the 1:1 state. The dynamic ensemble for a 2:1 complex, harboring a symmetrized stacked dimer bound to self-complementary DNA, is expected to sample symmetry-related configurations that are absent for the asymmetric 1:1 complex. In addition, a stacked dimer that removes substantial low-polarity surfaces from the solvent is compatible with the solute-specific preferential interactions

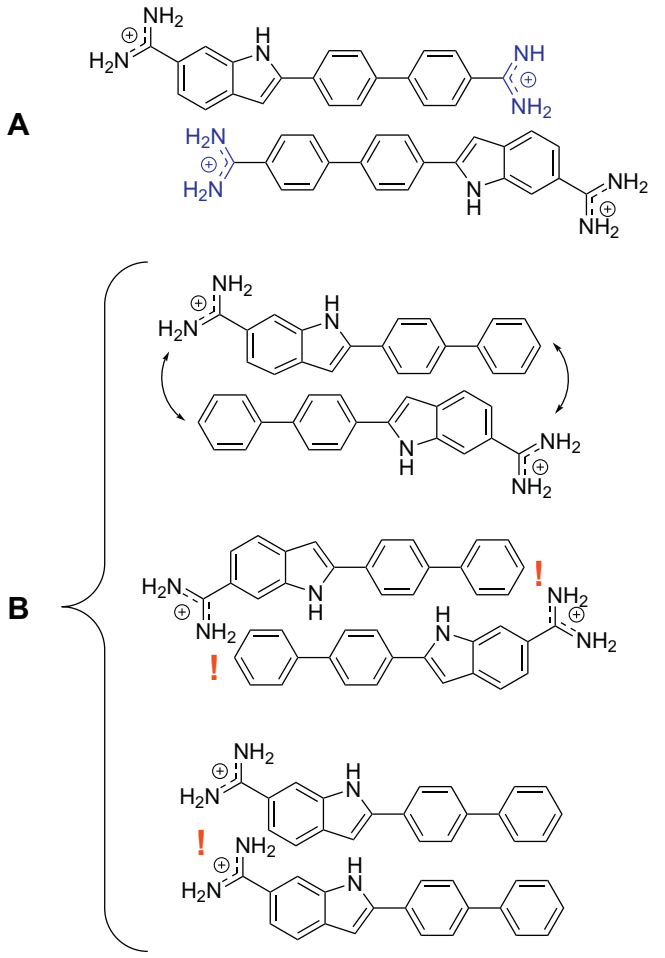

Fig. 10. A model for dimer formation by linear indole-biphenyl dications. As illustrative examples, the diamidine DB1883 and its mono-amidine analogue DB1944 are shown here, offset vertically in the plane of the page for presentation in two dimensions. A, An antiparallel stacked dimer of DB1883 is stabilized by π-stacking and cation-π interactions with the amidinium at each phenyl end (colored in blue), as well as molecular symmetry. B, Illustrative configurations of stacking by two DB1944 monocations. The equivalent cation-π interactions to those of DB1883 cannot be achieved by the off-axis amidinium at the indole end of DB1944 without less optimal geometries (marked by double-headed arrows) or steric clashes and electronic repulsion (red exclamation symbols). (For interpretation of the references to color in this figure legend, the reader is referred to the web version of this article.)

(DMSO, nicotinamide, MPD) observed with DB1804. The formal possibility of a 2:1 complex in the major groove is discounted by the susceptibility of the 2:1 complex to inhibition by netropsin, an established minor groove ligand, and the lack of evidence for an allosteric mechanism of inhibition.

The 5′-AATT-3′ motif, as found in A_2T_2, narrows into the midpoint of the sequence at the minor groove. To accommodate the 2:1 complex, induced perturbation in the structure of both DNA minor groove and ligand is therefore likely, with the possible consequence that additional charge neutralization is needed to maintain a compatible level of axial charge density in the complex. If an uptake of anions by the compound is coupled to cation (Na^+) release from the neutralization of DNA phosphates (as demonstrated by the monocations), the compensation could explain the apparent salt insensitivity of high-affinity binding to A_2T_2 by the two dications. Additional supporting evidence for mutual structural adjustment by DNA and ligand is found in the ~5-fold lower affinity of the 2:1 mode for DB1883, the more facile dimer in the absence of DNA, relative to DB1804. Such structural perturbations may

not be needed for the suboptimal DNA site in A_2CGT_2, for which the minor groove is expected to be wider relative to A_2T_2. Accordingly, A_2CGT_2 binding by DB1804 is salt sensitive and nearly as strong as binding to A_2T_2 at low salt (Fig. 6).

4.2. Functional implications of multiple binding modes for dications as transcriptional inhibitors

Translationally, minor groove-binding heterocyclic cations are promising agents as antimicrobials and other therapeutics [34], including recent success as inhibitors of transcription factors of major oncologic interest [35–37]. Their therapeutic potential in transcriptional regulation depends, mechanistically, on their ability to competitively inhibit protein/DNA interactions at the minor groove. In this respect, the susceptibility of both binding modes of DB1804 to inhibition by netropsin *at equilibrium* is significant, as the thermodynamic nature of the data assures that the reciprocal action also holds. In other words, minor groove binding as realized by netropsin can also be inhibited by both the high- and low-affinity binding modes of DB1804. The 2:1 complex is therefore a functionally effective binding mode as far as minor groove inhibition is concerned, even if the structure of dimeric DB1804 (and, by extension, DB1883) in the minor groove is not definitively defined. Indeed, the high affinity of 2:1 binding (near 10^{-9} M under physiologically saline conditions) relative to the two monocationic analogs supports the 2:1 mode as a desirable characteristic in the molecular design of inhibitors with this scaffold.

5. Conclusion

We evaluated the solution binding modes of the two linear indole-biphenyl dications DB1804 (ditetrahydropyrimidine) and DB1883 (diamidine) as well as their respective monocations DB2627 and DB1944. In dilute solution, a dimeric DNA binding mode is accessible only to the dications. The monocationic analogues, which differ from the dications only by the absence of one cationic terminus, exhibit a single 1:1 binding mode typical of minor groove binders of this general class. These structure-binding relationships reflect cation-π stacking of a linear indole-biphenyl cation core that is not typically observed with isohelical heterocyclic compounds.

Acknowledgements

The authors thank Drs. W. David Wilson and Samer Gozem for helpful discussion and suggestions. We also thank the reviewers for their suggestions and insights. N.E. was supported by a 2017 Barry Goldwater Scholarship. This investigation was funded by National Science Foundation grant MCB 15451600 to G.M.K.P.

Appendix A. Supplementary data

Supplementary data to this article can be found online at https://doi.org/10.1016/j.bpc.2018.11.004.

References

[1] D. Goodsell, R.E. Dickerson, Isohelical analysis of DNA groove-binding drugs, J. Med. Chem. 29 (1986) 727–733.
[2] P.B. Dervan, Molecular recognition of DNA by small molecules, Bioorg. Med. Chem. 9 (2001) 2215–2235.
[3] B. Nguyen, M.P. Lee, D. Hamelberg, A. Joubert, C. Bailly, R. Brun, S. Neidle, W.D. Wilson, Strong binding in the DNA minor groove by an aromatic diamidine with a shape that does not match the curvature of the groove, J. Am. Chem. Soc. 124 (2002) 13680–13681.
[4] B. Nguyen, D. Hamelberg, C. Bailly, P. Colson, J. Stanek, R. Brun, S. Neidle, W.D. Wilson, Characterization of a Novel DNA Minor-Groove complex, Biophys. J. 86 (2004) 1028–1041.
[5] Y. Miao, M.P. Lee, G.N. Parkinson, A. Batista-Parra, M.A. Ismail, S. Neidle, D.W. Boykin, W.D. Wilson, Out-of-shape DNA minor groove binders: induced fit interactions of heterocyclic dications with the DNA minor groove, Biochemistry 44 (2005) 14701–14708.
[6] Y. Liu, A. Kumar, S. Depauw, R. Nhili, M.H. David-Cordonnier, M.P. Lee, M.A. Ismail, A.A. Farahat, M. Say, S. Chackal-Catoen, A. Batista-Parra, S. Neidle, D.W. Boykin, W.D. Wilson, Water-mediated binding of agents that target the DNA minor groove, J. Am. Chem. Soc. 133 (2011) 10171–10183.
[7] F.A. Tanious, W. Laine, P. Peixoto, C. Bailly, K.D. Goodwin, M.A. Lewis, E.C. Long, M.M. Georgiadis, R.R. Tidwell, W.D. Wilson, Unusually strong binding to the DNA minor groove by a highly twisted benzimidazole diphenylether: induced fit and bound water, Biochemistry 46 (2007) 6944–6956.
[8] D. Wei, W.D. Wilson, S. Neidle, Small-molecule binding to the DNA minor groove is mediated by a conserved water cluster, J. Am. Chem. Soc. 135 (2013) 1369–1377.
[9] R. Nanjunda, W.D. Wilson, Binding to the DNA minor groove by heterocyclic dications: from AT-specific monomers to GC recognition with dimers, Curr. Protoc. Nucleic Acid Chem. 51 (2012) 8.8.1–8.8.20 (Unit8 8).
[10] N. Erlitzki, K. Huang, S. Xhani, A.A. Farahat, A. Kumar, D.W. Boykin, G.M. Poon, Investigation of the electrostatic and hydration properties of DNA minor groove-binding by a heterocyclic diamidine by osmotic pressure, Biophys. Chem. 231 (2017) 95–104.
[11] D.C. Stephens, H.M. Kim, A. Kumar, A.A. Farahat, D.W. Boykin, G.M.K. Poon, Pharmacologic efficacy of PU.1 inhibition by heterocyclic dications: a mechanistic analysis, Nucleic Acids Res. 44 (2016) 4005–4013.
[12] W.M. Haynes, CRC Handbook of Chemistry and Physics, 94th Ed., CRC Press, Boca Raton, Florida, 2013.
[13] M.T. Record Jr., C.F. Anderson, T.M. Lohman, Thermodynamic analysis of ion effects on the binding and conformational equilibria of proteins and nucleic acids: the roles of ion association or release, screening, and ion effects on water activity, Q. Rev. Biophys. 11 (1978) 103–178.
[14] M.T. Record, T.M. Lohman, A semiempirical extension of polyelectrolyte theory to the treatment of oligoelectrolytes: Application to oligonucleotide helix-coil transitions, Biopolymers 17 (1978) 159–166.
[15] M.L. Bleam, C.F. Anderson, M.T. Record, Relative binding affinities of monovalent cations for double-stranded DNA, Proc. Natl. Acad. Sci. U. S. A. 77 (1980) 3085–3089.
[16] L.A. Marky, K.J. Breslauer, Origins of netropsin binding affinity and specificity: correlations of thermodynamic and structural data, Proc. Natl. Acad. Sci. U. S. A. 84 (1987) 4359–4363.
[17] Z. Lakos, Á. Szarka, L. Koszorús, B. Somogyi, Quenching-resolved emission anisotropy: a steady state fluorescence method to study protein dynamics, J. Photoch. Photobiol. B 27 (1995) 55–60.
[18] M.L. Kopka, C. Yoon, D. Goodsell, P. Pjura, R.E. Dickerson, Binding of an antitumor drug to DNA: Netropsin and C-G-C-G-A-A-T-T-BrC-G-C-G, J. Mol. Biol. 183 (1985) 553–563.
[19] X. Chen, S.N. Mitra, S.T. Rao, K. Sekar, M. Sundaralingam, A novel end-to-end binding of two netropsins to the DNA decamers d(CCCCCIIIII)2, d(CCCBr5CCIIIII) 2and d(CBr5CCCCIIIII)2, Nucleic Acids Res. 26 (1998) 5464–5471.
[20] G. Burckhardt, H. Votavova, J. Sponar, G. Luck, C. Zimmer, Two binding modes of netropsin are involved in the complex formation with poly(dA-dT).Poly(dA-dT) and other alternating DNA duplex polymers, J. Biomol. Struct. Dyn. 2 (1985) 721–736.
[21] M.W. Freyer, R. Buscaglia, D. Cashman, S. Hyslop, W.D. Wilson, J.B. Chaires, E.A. Lewis, Binding of netropsin to several DNA constructs: evidence for at least two different 1:1 complexes formed from an –AATT-containing ds-DNA construct and a single minor groove binding ligand, Biophys. Chem. 126 (2007) 186–196.
[22] J. Lah, I. Drobnak, M. Dolinar, G. Vesnaver, What drives the binding of minor groove-directed ligands to DNA hairpins? Nucleic Acids Res. 36 (2008) 897–904.
[23] M. Durand, N.T. Thuong, J.C. Maurizot, Binding of netropsin to a DNA triple helix, J. Biol. Chem. 267 (1992) 24394–24399.
[24] Y.W. Park, K.J. Breslauer, Drug binding to higher ordered DNA structures: netropsin complexation with a nucleic acid triple helix, Proc. Natl. Acad. Sci. U. S. A. 89 (1992) 6653–6657.
[25] C. Zimmer, C. Marck, W. Guschlbauer, Z-DNA and other non-B-DNA structures are reversed to B-DNA by interaction with netropsin, FEBS Lett. 154 (1983) 156–160.
[26] L. Minchenkova, C. Zimmer, Reversion of the B to A transition of DNA induced by specific interaction with the oligopeptide distamycin A, Biopolymers 19 (1980) 823–831.
[27] B. Nguyen, C. Tardy, C. Bailly, P. Colson, C. Houssier, A. Kumar, D.W. Boykin, W.D. Wilson, Influence of compound structure on affinity, sequence selectivity, and mode of binding to DNA for unfused aromatic dications related to furamidine, Biopolymers 63 (2002) 281–297.
[28] L. Wang, C. Bailly, A. Kumar, D. Ding, M. Bajic, D.W. Boykin, W.D. Wilson, Specific molecular recognition of mixed nucleic acid sequences: an aromatic dication that binds in the DNA minor groove as a dimer, Proc. Natl. Acad. Sci. U. S. A. 97 (2000) 12–16.
[29] C. Bailly, C. Tardy, L. Wang, B. Armitage, K. Hopkins, A. Kumar, G.B. Schuster, D.W. Boykin, W.D. Wilson, Recognition of ATGA sequences by the unfused aromatic dication DB293 forming stacked dimers in the DNA minor groove, Biochemistry 40 (2001) 9770–9779.
[30] M. Munde, A. Kumar, R. Nhili, S. Depauw, M.H. David-Cordonnier, M.A. Ismail, C.E. Stephens, A.A. Farahat, A. Batista-Parra, D.W. Boykin, W.D. Wilson, DNA minor groove induced dimerization of heterocyclic cations: compound structure, binding affinity, and specificity for a TTAA site, J. Mol. Biol. 402 (2010) 847–864.
[31] F.A. Tanious, D. Hamelberg, C. Bailly, A. Czarny, D.W. Boykin, W.D. Wilson, DNA sequence dependent monomer-dimer binding modulation of asymmetric benzimidazole derivatives, J. Am. Chem. Soc. 126 (2004) 143–153.
[32] D.A. Dougherty, The cation-pi interaction, Acc. Chem. Res. 46 (2013) 885–893.
[33] S. Wang, K. Aston, K.J. Koeller, G.D. Harris, N.P. Rath, J.K. Bashkin, W.D. Wilson, Modulation of DNA–polyamide interaction by β-alanine substitutions: a study of

positional effects on binding affinity, kinetics and thermodynamics, Org. Biomol. Chem. 12 (2014) 7523–7536.
[34] W.D. Wilson, B. Nguyen, F.A. Tanious, A. Mathis, J.E. Hall, C.E. Stephens, D.W. Boykin, Dications that target the DNA minor groove: compound design and preparation, DNA interactions, cellular distribution and biological activity, Curr. Med. Chem. Anticancer Agents 5 (2005) 389–408.
[35] I. Antony-Debre, A. Paul, J. Leite, K. Mitchell, H.M. Kim, L.A. Carvajal, T.I. Todorova, K. Huang, A. Kumar, A.A. Farahat, B. Bartholdy, S.R. Narayanagari, J. Chen, A. Ambesi-Impiombato, A.A. Ferrando, I. Mantzaris, E. Gavathiotis, A. Verma, B. Will, D.W. Boykin, W.D. Wilson, G.M. Poon, U. Steidl, Pharmacological inhibition of the transcription factor PU.1 in leukemia, J. Clin. Invest. 127 (2017) 4297–4313.
[36] M. Munde, S. Wang, A. Kumar, C.E. Stephens, A.A. Farahat, D.W. Boykin, W.D. Wilson, G.M. Poon, Structure-dependent inhibition of the ETS-family transcription factor PU.1 by novel heterocyclic diamidines, Nucleic Acids Res. 42 (2014) 1379–1390.
[37] R. Nhili, P. Peixoto, S. Depauw, S. Flajollet, X. Dezitter, M.M. Munde, M.A. Ismail, A. Kumar, A.A. Farahat, C.E. Stephens, M. Duterque-Coquillaud, W. David Wilson, D.W. Boykin, M.H. David-Cordonnier, Targeting the DNA-binding activity of the human ERG transcription factor using new heterocyclic dithiophene diamidines, Nucleic Acids Res. 41 (2013) 125–138.